A new reverse electrodialysis design strategy which significantly reduces the levelized cost of electricity

Citation: Weiner, Adam M., Ronan K. McGovern, and John H. Lienhard V. "A New Reverse Electrodialysis Design Strategy Which Significantly Reduces the Levelized Cost of Electricity." Journal of Membrane Science 493 (November 2015): 605–614.

As Published: http://dx.doi.org/10.1016/j.memsci.2015.05.058

Publisher: Elsevier

Persistent URL: http://hdl.handle.net/1721.1/104000

Version: Author's final manuscript: final author's manuscript post peer review, without publisher's formatting or copy editing

A new reverse electrodialysis design strategy which significantly reduces the levelized cost of electricity

Adam M. Weiner[a], Ronan K. McGovern[a], John H. Lienhard V[a]

[a]*Center for Clean Water and Clean Energy, Department of Mechanical Engineering*
Massachusetts Institute of Technology, Cambridge, MA 02139 USA

Abstract

We develop a framework for choosing the optimal load resistance, feed velocity, and residence time for a reverse electrodialysis stack based on minimizing the levelized cost of electricity. The optimal load resistance maximizes the gross stack power density and results from a trade-off between stack voltage and stack current. The primary trade-off governing the optimal feed velocity is between stack pumping power losses which reduce the net power density and concentration polarization losses which reduce the gross stack power density. Lastly, the primary trade-off governing the optimal residence time is between the capital costs of the stack and pretreatment system. Implementing our strategy, we show that a smaller load resistance and feed velocity as well as a larger residence time than what is currently proposed in the literature reduces costs by over 40%. Despite these reductions, reverse electrodialysis remains more costly than other renewable technologies.

Keywords: reverse electrodialysis, salinity gradient power, renewable energy, levelized cost of electricity

1. Introduction

A reverse electrodialysis stack consists of alternating layers of anion and cation exchange membranes sandwiched between two electrodes, which are connected in series to an external load resistor. Diluate and concentrate feeds are pumped between the layers, facilitating ion transfer along the membrane length and converting the chemical potential stored in the salinity gradient to electrical work. In the literature, aspects of the overall system performance have been improved through the introduction of smaller channel heights [1], profiled membranes [2], and ion conductive spacers [3].

Other improvements result from optimizing RED stack design parameters. Studies to date have focused on maximizing performance parameters such as stack power density [1, 3–5], net power density (stack power density net of pumping power) [1, 6], efficiency (or power per unit water) [4, 5], and response product (efficiency times net power density) [7]. By contrast, our study represents the first cost-based optimization of RED stack design parameters. Specifically, we determine the optimal load resistance, residence time (length divided by feed velocity), and feed velocity based on minimizing the levelized cost of electricity produced. We show how the resulting cost-based design is different from the previous designs currently proposed in the literature. We also identify the important trade-offs using this approach.

The optimal load resistance is explained by considering the trade-off between stack current and stack voltage. In literature, the load resistance is most often chosen by setting it equal to the equivalent stack resistance, as in traditional impedance or load matching, to maximize the power density delivered by the stack (the gross power density) [1, 2, 8]. This approach, however, is not optimal because of salinity variations along the stack [4, 9]. We propose a more rigorous numerical maximization of the gross power density to determine the optimal load resistance, showing analytically that the optimal load resistance is always smaller than the equivalent stack resistance. Additionally, we show that the load resistance which maximizes the gross power density also minimizes the levelized cost of electricity.

Another important trade-off is between power density and efficiency (or stack capital cost and pretreatment cost). Here, the relevant design parameters to consider are residence time, charge utilization, stack length, and feed velocity - two of which are independent. In a related study, Yip et al. [4] examined the effect of charge utilization on power density and efficiency separately, neglecting concentration polarization (or effectively keeping the feed velocity large). We argue that the most complete and intuitive approach is to consider the effect of velocity (holding residence time constant) and residence time (holding velocity constant) on the levelized cost of electricity with concentration polarization considered. Framing the opti-

Email addresses: aweiner@alum.mit.edu (Adam M. Weiner), mcgov@alum.mit.edu (Ronan K. McGovern), lienhard@mit.edu (John H. Lienhard V)

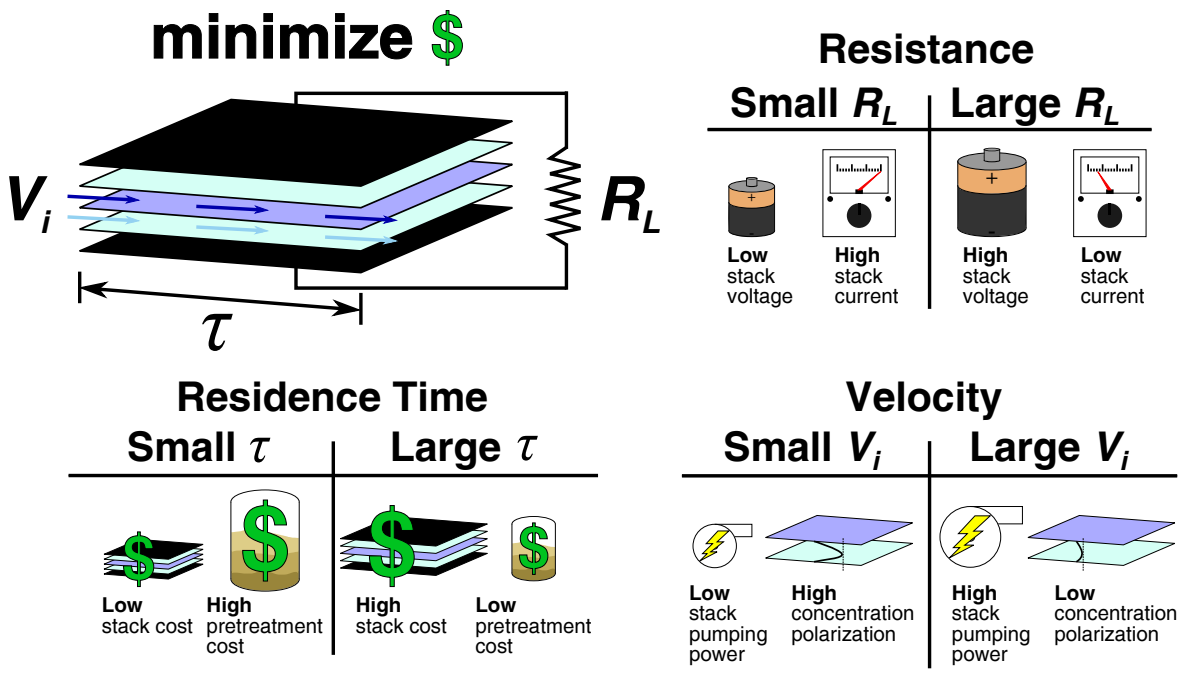

Figure 1: The primary trade-offs associated with determining the optimal load resistance R_L, optimal inlet feed velocity V_i, and optimal residence time τ which minimize the levelized cost of electricity.

mization in terms of velocity and residence time decouples the capital cost versus pretreament cost trade-off from another important trade-off - concentration polarization losses versus pumping power losses. The result is a more intuitive understanding of the optimal RED stack design.

Based on the consideration of these trade-offs (see Fig. 1), we find that the optimal load resistance and feed velocity is actually significantly smaller and the optimal residence time is significantly larger than values reported in the literature.

2. Methodology

Figure 2 illustrates our recommended optimization approach for designing an RED stack. We design a step-wise approach for two reasons. First, the step-wise approach clearly quantifies the trade-offs in determining the optimal parameters. Second, the step-wise optimization simplifies the procedure for experimental validation by reducing the parameter space. We show that the loss in cost savings resulting from a step-wise optimization is negligible, and only one iteration is sufficient.

First we fix the residence time τ to an arbitrary value significantly larger than a critical residence time τ_c. While holding the residence time fixed, we minimize the levelized cost of electricity with respect to the superficial feed velocity and load resistance. Because the residence time is fixed, the stack length is implicitly varied as well. We show that this optimization step is equivalent to maximizing the gross power density with respect to the load resistance and maximizing the net power density with respect to the feed velocity. Then we fix the feed velocity and minimize the cost with respect to residence time and load resistance. Again, the stack length is implicitly varied in this step. Together, the optimal feed velocity and residence time yield the optimal stack length.

In our analysis, we hold the diluate and concentrate channel heights constant and equal at 100 μm - the optimal channel height with respect to net power density identified by Vermaas et al. [1]. While smaller channel heights increase the gross power density, they also increase pumping power losses as well as manufacturing difficulty. Larger channel heights significantly reduce the gross power density, and the sensitivity of our results to channel height is explored in Sect. 6.1. We set the feed velocities equal and channel heights equal to simplify the system design. We suggest that the greatest cost reductions can be achieved through optimizing the load resistance, residence time, and feed velocity.

The first step in calculating the levelized cost of electricity for the optimization procedure is to model the net power density of the system - the gross power density less the pumping power density consumed in the pretreatment (PT) system and the stack. Our method is illustrated in Fig. 3. In Sect. 3, we show that the load resistance which maximizes the gross power density also minimizes the levelized cost of electricity. Hence, in modeling the gross power density we always maximize with respect to the load resistance.

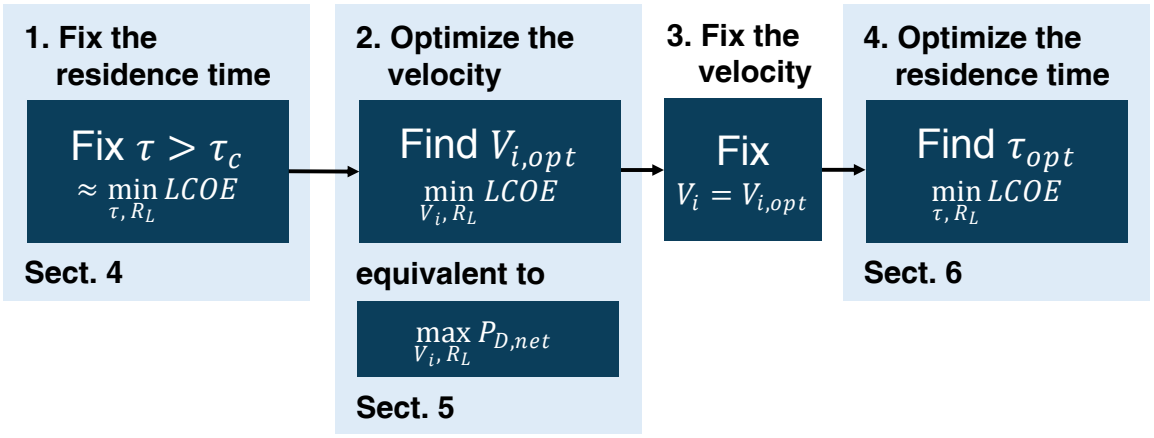

Figure 2: An optimization method for RED stack design, where τ is the residence time and τ_c is the critical residence time, $LCOE$ is the levelized cost of electricity, R_L is the load resistance, and V_i is the superficial inlet feed velocity.

The gross power density model itself is of an unsegmented-electrode RED stack, validated with experimental results from the literature. The model is one-dimensional, accounting for streamwise variations in salinities, membrane potentials, and channel resistances along the stack. We base the model for pumping power consumed in the pretreatment system and stack on systems reported in the literature, and all equations were solved numerically using a quadratic approximation method in Engineering Equation Solver [10].

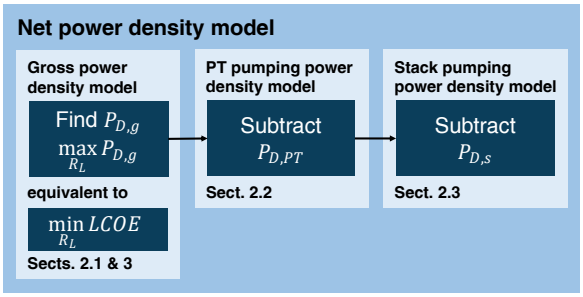

Figure 3: The net power density of the system $P_{D,net}$ is the gross power density $P_{D,g}$ supplied by the stack, continuously maximized with respect to the load resistance R_L, less the power densities consumed in pumping the feed through the pretreatment system $P_{D,PT}$ and stack $P_{D,s}$.

2.1. Model for gross power density

Figure 4 shows how the circuit was modeled to determine the gross power density. An RED cell pair is divided along the length L into N discrete segments to capture stream-wise variations in concentration. Each segment is connected in parallel via the unsegmented electrodes on either side, and the electrodes are joined in series with a single, external load resistor. We model neither ionic shortcut currents nor voltage losses to chemical reactions at the electrodes. In stacks with many cell pairs in series, the voltage loss at the electrodes is negligible relative to the sum of the membrane potentials.

Because the concentration of the diluate and concentrate streams vary along the stack length, each segment has an associated local electromotive force (EMF) ε_n effectively connected in series with membrane surface resistances ($\bar{r}_{\mathrm{AEM}}$ and $\bar{r}_{\mathrm{CEM}}$) and local channel resistances ($\bar{r}_{d,n}$ and $\bar{r}_{c,n}$). We assume the membrane surface resistances are constant along the length.

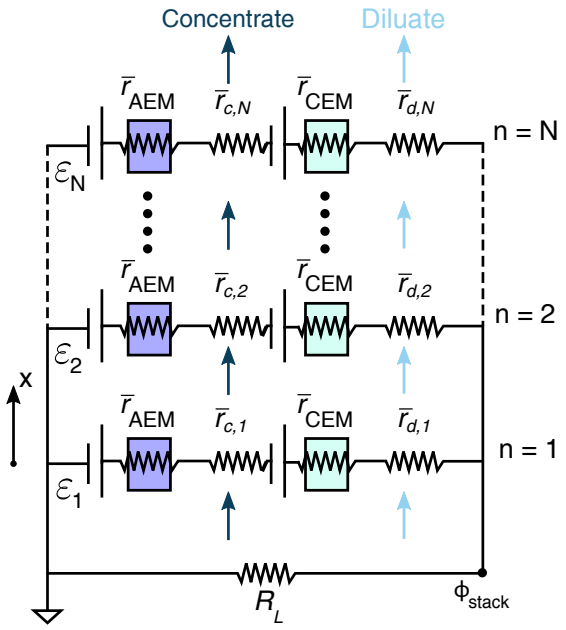

Figure 4: A circuit model for the one-dimensional, unsegmented-electrode RED stack which accounts for streamwise variations in concentration.

The local EMFs ε_n are computed from the local chemical potential differences across the membranes:

$$\varepsilon_n = \frac{t_s}{F}\left(\mu_{s,c,m,n} - \mu_{s,d,m,n}\right) + \frac{t_w}{F}\left(\mu_{w,c,m,n} - \mu_{w,d,m,n}\right) \quad (1)$$

where t_s is the salt transport number, F is Faraday's constant, $\mu_{s,c,m,n}$ is the local salt chemical potential at the membrane surface on the concentrate side, and $\mu_{s,d,m,n}$ is the local salt chemical potential at the membrane surface on the diluate side. The difference in concentration between the channel bulk and membrane surface due to concentration polarization was computed using a convection-diffusion model [11] (diluate example shown):

$$C_{d,m,n} - C_{d,n} = \frac{2h_d}{\mathrm{Sh}_{d,n}} \frac{j_{D,n}}{F} \frac{(\bar{T}_{cu} - t_{cu})}{D_{\mathrm{NaCl}}} \quad (2)$$

where $C_{d,m,n}$ is the local diluate concentration at the membrane, $C_{d,n}$ is the local diluate concentration in the bulk, $j_{D,n}$ is the local current density (see Eq. 5 below), h_d is the diluate channel height, t_{cu} is the counter-ion transport number (≈0.5 for anions and cations), and D_{NaCl} is the diffusion coefficient of salt through the bulk. $\bar{T}_{cu}$ is the integral counter-ion transport number in the membrane, accounting for migration and diffusion [12]:

$$\bar{T}_{cu} \approx \frac{t_s + 1}{2} \quad (3)$$

$\mathrm{Sh}_{d,n}$ is the local Sherwood number, modeled by Kuroda et al. [13] (diluate example shown):

$$\mathrm{Sh}_{d,n} = K_m \mathrm{Re}_{D_h,d,n}^{1/2} \mathrm{Sc}_{d,n}^{1/3} \quad (4)$$

where K_m is the Kuroda constant, $\mathrm{Re}_{D_h,d,n}$ is the local Reynolds number based on the hydraulic diameter D_h and the superficial velocity $V_{d,n}$, and $\mathrm{Sc}_{d,n}$ is the local Schmidt number. The local current density was modeled as:

$$j_{D,n} = \frac{\varepsilon_n - \phi_{\mathrm{stack}}}{\bar{r}_{tot,n}} \quad (5)$$

where ϕ_{stack} is the stack voltage and $\bar{r}_{tot,n}$ is the total local surface resistance, given by [6]:

$$\bar{r}_{tot,n} = \bar{r}_{\mathrm{AEM}} + \bar{r}_{\mathrm{CEM}} + \bar{r}_{d,n} + \bar{r}_{c,n} \quad (6)$$

The local channel resistances $\bar{r}_{d,n}$ and $\bar{r}_{c,n}$ are modeled as [6] (diluate example shown):

$$\bar{r}_{d,n} = \frac{h_d}{\epsilon^2 \kappa} \quad (7)$$

where ϵ is the spacer porosity and κ is the solution conductivity - the bulk concentration times the solution conductance [14]. An open spacer is described by a mask factor β of zero and a spacer porosity ϵ of unity. The opposite is true for a solid spacer [6]. Summing up the local current densities $j_{D,n}$ and applying Kirchoff's Current Law yields an expression for the total stack voltage ϕ_{stack}:

$$\phi_{\mathrm{stack}} = \frac{\sum \frac{\varepsilon_n}{\bar{r}_{tot,n}} A_n}{\frac{1}{R_L} + \sum \frac{1}{\bar{r}_{tot,n}} A_n} \quad (8)$$

where A_n is the area of a segment.

The local molar salt and water fluxes $J_{s,n}$ and $J_{w,n}$ transported into the diluate channel are modeled as the sum of migration and diffusion terms based on an approach taken by Fidaleo and Moresi [15]:

$$J_{s,n} = t_s \frac{j_{D,n}}{F} + L_s(C_{c,m,n} - C_{d,m,n}) \quad (9)$$

$$J_{w,n} = t_w \frac{j_{D,n}}{F} - L_w(\pi_{c,m,n} - \pi_{d,m,n}) \quad (10)$$

where L_s is the overall salt permeability (in m/s), t_w is the water transport number, L_w is the overall water permeability (in mol/bar-m^2-s), and $\pi_{m,n}$ is the local osmotic pressure at the membrane surface [16]. Finally, the gross power density $P_{D,g}$ is given by:

$$P_{D,g} = \frac{\phi_{\mathrm{stack}}^2}{R_L w l} \quad (11)$$

where w is the stack width and l is the stack length.

The constants used in the model are compiled in Appendix E. To determine the salt and water permeabilities, salt transport number, and Kuroda constant, the model is fit to experimental data [1], see Appendix A.

2.2. Model for pretreatment system pumping

The pretreatment system is based on a setup suggested by Post et al. [17]. It consists of coarse media-filtration in the form of two rotating drum filters, with light chlorination (1 ppm). We assume a constant, average head loss H of 3.66 m through each drum. The pressure drop is multiplied by the flow rate and divided by the total membrane area to compute a consumed power density for pumping each feed (concentrate and diluate) through the pretreatment system $P_{D,PT}$:

$$P_{D,PT} = \frac{\rho g H h}{\tau} \quad (12)$$

where ρ is the feed density, g is the acceleration due to gravity, and τ is the residence time.

2.3. Model for stack pumping

The energy cost associated with pumping the concentrate and diluate through the stack is also computed as a power density $P_{D,s}$. The pressure drop across the stack is fit to experimental data [1], see Appendix D. Multiplying by the flow rates and dividing by the total membrane area yields the following expression:

$$P_{D,s} = \frac{K_p \mu V_i^2}{h} \tag{13}$$

where K_p is a fit parameter and μ is the feed viscosity.

2.4. Model for system cost

The cost model was based on the approach taken for electrodialysis by McGovern et al. [18]. The levelized cost of electricity *LCOE* is defined as the net present value, NPV, of the combination of the RED system's capital cost, the pre-treatment system's capital cost and the pre-treatment system's lifetime operating expenses (excluding energy), divided by the net power output times the capital amortization factor CAF:

$$LCOE = \frac{\text{NPV}}{(P_{D,\text{net}} wl)\text{CAF}} \tag{14}$$

where the net power density $P_{D,\text{net}}$ is given by:

$$P_{D,\text{net}} = P_{D,g} - P_{D,PT} - P_{D,s} \tag{15}$$

and the capital amortization factor is given by:

$$\text{CAF} = \frac{1}{r}\left[1 - \left(\frac{1}{1+r}\right)^{\Gamma}\right] \tag{16}$$

We assume a plant life of 20 years (Γ in periods) and an annualized cost of capital r of 6% [17]. The net present value consists of a capital contribution for the RED stack and a capital contribution for the pretreatment system. Bundled into the pretreatment capital cost is an operating expense contribution, namely chemical costs associated with pretreatment:

$$\text{NPV} = K_{mem} wl + 2K_{PT} V_i hw \tag{17}$$

where K_{PT} is the pretreatment system capital cost figure in \$/(m^3/day), and K_{mem} is the RED stack capital cost figure in \$/m^2.

We use a capital cost figure for the pretreatment system K_{PT} of 20 \$/(m^3/day), which includes operating costs. The capital cost of the pretreatment system is computed by dividing the total construction costs by the operating flux of the system developed by Post et al. [17]. The chemical cost figure associated with light chlorination is 0.33 \$/kg [19].

We use a capital cost figure for the RED stack K_{mem} of 750 \$/m^2 [20, 21]. Here, we assume that RED capital costs scale solely with membrane area and are similar to ED capital costs. This value is a total installed capital cost. It includes the total cost of all equipment as well as installation costs and profits for equipment manufacturers and installers. For comparison, this total unit capital cost is significantly higher than previously reported membrane capital costs (€50/m^2 [22]) and also higher than previously reported total investment costs of \$100/m^2 [23]. Simplifying the expression for the levelized cost of electricity and rewriting it in terms of the residence time τ instead of the length yields the following:

$$LCOE = \frac{1}{P_{D,\text{net}}}\left(\frac{K_{mem}}{\text{CAF}} + 2\frac{K_{PT} h}{\tau \text{CAF}}\right) \tag{18}$$

The most intuitive approach in the cost-based optimization is to frame everything in terms of residence time and velocity as opposed to any other pair of independent variables chosen among residence time, charge utilization, stack length, and feed velocity. In Eq. 18, fixing the residence time and optimizing for velocity (Steps 1 and 2, Fig. 2) simplifies the objective from minimizing cost to maximizing net power density. Additionally, to first order, fixing the residence time fixes total salt transport through the membrane. Hence, the gross power density rises with velocity, solely because concentration polarization losses decrease.

3. Dependence of power density and cost on load resistance

The load resistance which minimizes the levelized cost of electricity also maximizes the gross power density, because all other terms in the levelized cost (Eq. 18) and net power density are constant with respect to load resistance. The primary trade-off determining the cost-effective load resistance is therefore between a high stack voltage and high stack current. According to Eq. 8, the stack voltage increases with increasing load resistance. At the same time, the local stack currents $j_{D,n}$ decrease according to Eq. 5 - primarily because of the increase in stack voltage.

Figure 5 shows how the gross power density varies with a dimensionless load resistance $\Theta = R_L/R_{eq}$ holding all other parameters constant. R_{eq} is an equivalent total stack resistance (technically defined as the Thévenin equivalent resistance of the circuit depicted in Fig. 4). At low Θ, large gains in stack voltage with increasing load resistance outweigh small reductions in stack current; the gross power density increases. Beyond the optimal Θ, the reductions in stack current outweigh the gains in stack voltage; the gross power density decreases.

Figure 6 shows how the levelized cost of electricity varies with dimensionless load resistance, confirming that the load resistance which maximizes the gross power density also minimizes the levelized cost of electricity. The optimal load resistance is 0.12 Ω per cell pair.

Interestingly, Figs. 5 and 6 show that the optimal load resistance is *smaller* than the equivalent total stack resistance (i.e. $\Theta_{opt} < 1$). If traditional load matching were optimal, $\Theta_{opt} = 1$ would maximize the gross power density. In Appendix B, we prove that the optimal load resistance is always smaller than the

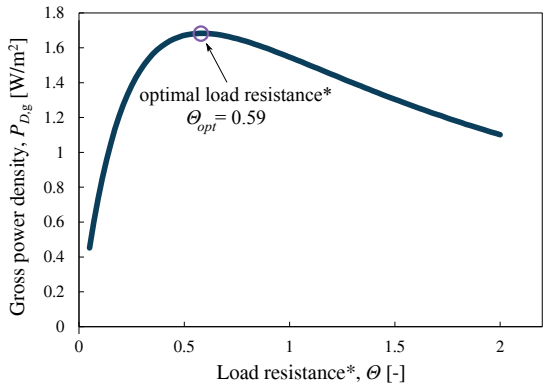

Figure 5: The load resistance which maximizes the gross power density is smaller than the equivalent stack resistance. The feed velocity and residence time are held constant at 0.5 cm/s and 20 s, respectively. The inlet diluate feed salinity is 1,000 ppm and the inlet concentrate feed salinity is 35,000 ppm.

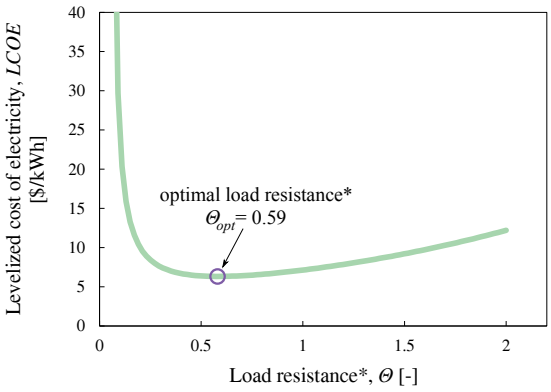

Figure 6: The load resistance which maximizes the gross power density also minimizes the levelized cost of electricity. The inlet diluate feed salinity is 1,000 ppm and the inlet concentrate feed salinity is 35,000 ppm.

equivalent stack resistance, regardless of the feed velocity or residence time chosen. Choosing the optimal load resistance versus simply load matching reduces the levelized cost of electricity by more than 30%.

4. Step 1: Fix the residence time

Initially, we fix the residence time to 20 s before computing the optimal feed velocity. We fix the residence time first, as opposed to the feed velocity, because beyond a critical residence time τ_c costs are relatively insensitive to changes in residence time (see Fig. 7). The rapid fall in cost at low residence times is caused by a significant rise in the net power density. At low residence times, the large pretreatment pumping power density dominates the gross power density output of the stack, driving the net power density to zero (see Eq. 12). At larger residence times, the pretreatment pumping power density is small compared to the gross power density of the stack. Costs rise mildly, primarily because the gross power density decreases mildly with residence time. For this configuration, a residence time of 20 s is situated comfortably beyond the critical residence time for a wide range of velocities. We will return to this trade-off in Sect. 6.

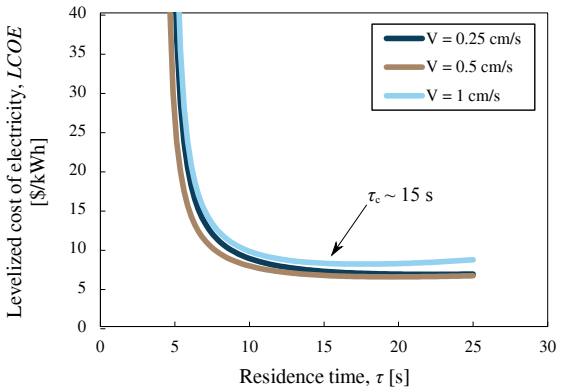

Figure 7: The dependence of levelized cost of electricity on residence time for a range of velocities.

5. Step 2: Optimize the velocity

With a fixed residence time, we minimize the levelized cost of electricity with respect to the inlet feed velocity V_i. Figure 8 shows the gross power density and pumping losses through the pretreatment system and stack when varying only the feed velocity. Figure 9 shows the resulting net power density. We find that a velocity of 0.46 cm/s minimizes the levelized cost of electricity for a typical seawater/river water configuration. The levelized cost of electricity is 6.33 $/kWh.

Equation 18 shows that with a fixed residence time, the cost-effective feed velocity simply maximizes the net power density. The pumping power losses through the pretreatment system $P_{D,PT}$ (Eq. 12) and, to first order, the rate of salt transport are constant with velocity when residence time is fixed. Therefore the primary trade-off in determining the optimal feed velocity is between concentration polarization losses in the gross power density and pumping power losses through the stack.

At low velocities, the losses due to concentration polarization are highly non-linear. Marginal increases in feed velocity result in large gross power density gains which outweigh increased pumping losses through the stack; the net power density rises with increasing feed velocity. At high velocities, the gross power density gains level off as the concentration polarization losses approach linearity. Pumping power losses through the stack dominate, driving the net power density down. At the maximum net power density, the curvature of the plot is sufficiently small that velocities within 20% of the optimum reduce the net power density by less than 1%. With a fixed residence time, the levelized cost of electricity varies inversely with the net power

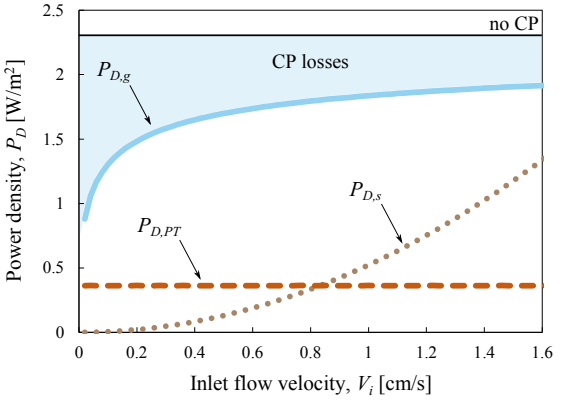

Figure 8: The residence time is fixed, and we vary the feed velocity. The gross power density $P_{D,g}$ and the power density consumed for pumping through the stack $P_{D,s}$ and pretreatment system $P_{D,PT}$ are shown. Gross power density losses arising from concentration polarization are shaded in light blue.

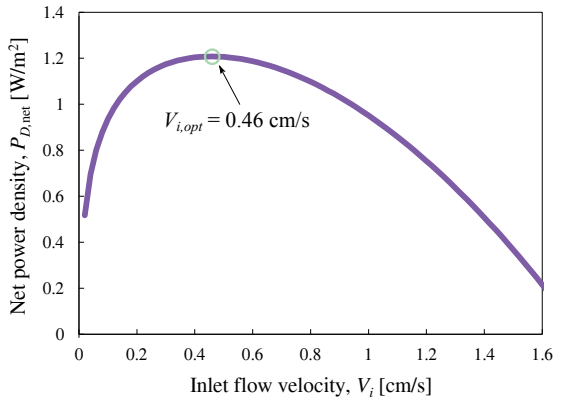

Figure 9: The residence time is fixed, and we vary the feed velocity. The net power density $P_{D,\text{net}}$ and the optimal feed velocity $V_{i,opt}$ are shown.

density, see Fig. 10. Velocities within 20% of the optimum reduce the levelized cost of electricity by less than 1% as well.

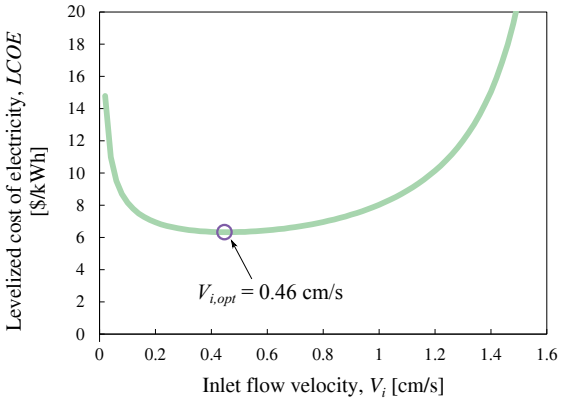

Figure 10: The residence time is fixed, and we vary the feed velocity. The levelized cost of electricity $LCOE$ and the optimal feed velocity $V_{i,opt}$ are shown.

The optimal feed velocity is significantly smaller than what is proposed in the literature. For a 10 cm long stack, an optimal feed velocity of 1 cm/s was found [1]. The optimization procedure consisted of fixing the stack length and measuring the net power density (not including the required pumping power through the pretreatment system) for different feed velocities, as opposed to optimizing both length and velocity with respect to levelized cost.

6. Step 4: Optimize the residence time

The velocity is fixed to 0.46 cm/s, and we minimize the levelized cost of electricity with respect to residence time. Unlike the optimal velocity, the optimal residence time does not simply maximize the net power density. Instead, the optimal residence time balances a trade-off between both the stack and pretreatment capital costs (see Eq. 18). We find that a residence time of 19.9 s minimizes the levelized cost of electricity for the typical seawater/river water stack. With an optimal velocity of 0.46 cm/s, this corresponds to an optimal stack length of 9.2 cm. The levelized cost of electricity is 6.33 $/kWh.

Figure 11 shows how the gross power density and pumping losses through the pretreatment system and stack vary with residence time, and Fig. 12 shows the resulting net power density. The residence time which maximizes the net power density τ^* weighs the trade-off between the gross power density and the pretreatment pumping power. The gross power density decreases with increasing residence time, because more salt is transported, reducing the average salinity gradient and local EMFs. On the other hand, pumping power density losses through the pretreatment system decrease with increasing residence time, because the losses are spread over a larger stack. A residence time of 19.2 s maximizes the net power density.

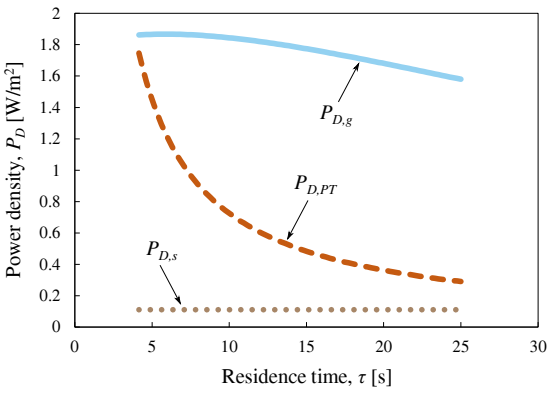

Figure 11: The velocity is fixed and the residence time is varied. The gross power density $P_{D,g}$ and the power density consumed for pumping through the stack $P_{D,s}$ and pretreatment system $P_{D,PT}$ are shown.

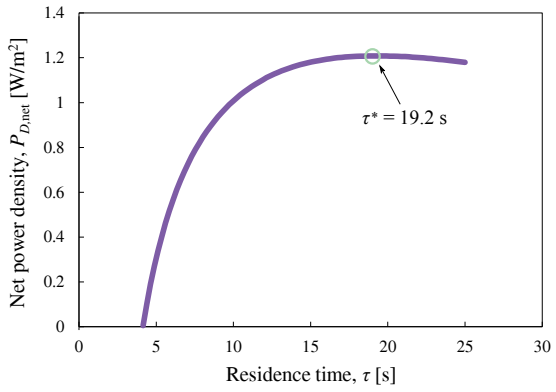

Figure 12: The velocity is fixed and the residence time is varied. The net power density $P_{D,\text{net}}$ and the residence time which maximizes the net power density τ^* are shown.

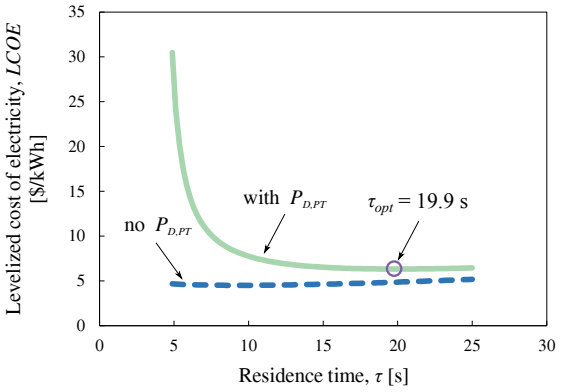

Figure 13: The velocity is fixed and the residence time is varied. We plot the levelized cost of electricity $LCOE$ with and without the pretreatment pumping power $P_{D,PT}$ considered. The optimal residence time τ_{opt} is larger than the one which maximizes the net power density τ^*.

Figure 13 shows the levelized cost of electricity $LCOE$ with and without the pretreatment pumping power $P_{D,PT}$ considered. The optimal residence time τ_{opt} (with $P_{D,PT}$ considered) is 19.9 s. The optimal residence time τ_{opt} is larger than τ^*, because the pretreatment capital costs decrease with increasing residence time (see Eq. 18). When the pretreatment pumping power is considered, τ^* and τ_{opt} are both higher, because these losses are very costly at low residence times.

We compute an optimal residence time that is greater than what is found in the literature. The literature suggests an optimal residence time of 8 s for a similar stack configuration [6]. We find a longer residence time to be optimal, because we consider both pumping losses and capital costs associated with the pretreatment system. The large residence time results in an optimal stack length which is slightly smaller than what is currently advocated in the literature. While on the face of it, the optimal stack length is only slightly different, this must be understood in the context of a significantly reduced feed velocity. The key insight is that more salt transport through the stack is optimal.

6.1. *Sensitivity of the optimal residence time and optimal feed velocity to select parameters*

We examine the sensitivity of the optimal residence time to the stack and pretreatment capital cost figures as well as the channel height by measuring the percent change in τ_{opt}, $P_{D,net}$, and $LCOE$ resulting from a 1% decrease in each parameter. For example, as shown in Table 1, a 1% decrease in the stack capital cost parameter K_{mem} results in a 0.02% increase in the optimal residence time τ_{opt}.

Table 1: Sensitivity of residence time to cost parameters and channel height

Parameter	$\Delta\tau_{opt}$	$\Delta P_{D,net}$	$\Delta LCOE$
K_{mem}	0.02%	0%	-1%
K_{PT}	-0.01%	0%	-0.02%
h	-1.5%	0.6%	-0.6%

Of the three design parameters considered in this study, the optimal residence time is the only one sensitive to cost parameters. As show in Table 1 the sensitivity is small. The optimal residence time is most sensitive to changes in the channel height.

The optimal feed velocity and optimal load resistance are also sensitive to changes in the channel height. We find that a 1% decrease in the channel height results in a -0.01% change in the optimal feed velocity and a 2.6% change in the optimal load resistance. The optimal residence time computed in Table 1 with the smaller channel height accounts for these changes.

We also examined the sensitivity of the results to membrane parameters. A 1% decrease in either L_s or L_w or the membrane resistances, $\bar{r}_{\text{AEM}}$ and $\bar{r}_{\text{CEM}}$, results in approximately a 0.01% decrease in the levelized cost of electricity.

7. Cost comparison to other design strategies

We model the levelized cost of electricity associated with different design strategies found in the literature and compare the results in Fig. 14. The costs shown are significantly higher than those generally reported in the RED literature, primarily because we use a larger stack capital cost figure which is based on average electrodialysis stack costs deployed commercially. More importantly, however, the design strategy presented in this study results in a more than 40% reduction in the levelized cost of electricity as compared to the leading strategy in the literature, where $P_{D,g} - P_{D,s}$ (the net power density not including the pretreatment pumping

power density) is maximized with respect to feed velocity and load resistance matching is employed [1]. No other strategy from the literature which we modeled, including maximizing the gross stack power density or maximizing the response product [7], resulted in a positive net power density output after pretreatment pumping power consumption was considered.

As an approximation to the strategy of minimizing the levelized cost of electricity, we consider maximizing the net power density in a form that includes the pumping power required to drive flow through the stack *and* the pretreatment system. For the range of cost parameters we considered, this approximate approach results in fairly comparable cost savings. This arises because the capital cost per unit net power produced dominates the levelized cost of electricity. We expect the cost savings associated with the approximate approach to diminish relative to the proposed approach as the capital cost per unit net power produced decreases relative to the pretreatment cost per unit net power produced.

As a further approximation, we maximize this net power density with load matching ($R_L = R_{eq}$) instead of load optimization ($R_L = R_{L,opt}$). We find this to be an inferior method, as the resulting levelized cost of electricity is over 12% higher than our proposed approach. Nevertheless, even after employing our proposed design approach the levelized cost of electricity remains nearly two orders of magnitude higher than current average electricity prices in the United States.

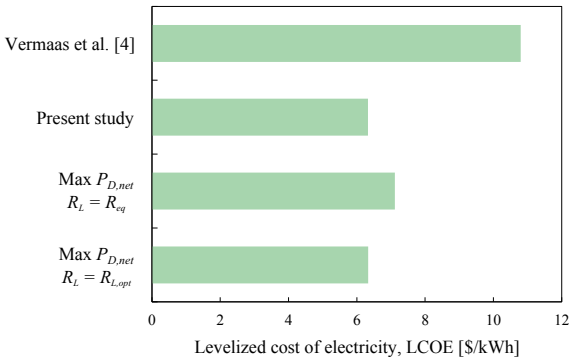

Figure 14: A cost comparison of different RED design strategies. The costs associated with design strategies where the gross power density is maximized or the response product is maximized were also modeled. Neither strategy resulted in a positive net power density output when pretreatment pumping power consumption was included.

8. Conclusions

An optimal stack design based on the minimization of the levelized cost of electricity produced consists of a smaller load resistance and feed velocity as well as a larger residence time than is currently described in the literature. We prescribe a load resistance of 0.12 Ω per cell pair, a feed velocity of 0.46 cm/s, and a residence time of 19.9 s for the typical seawater/freshwater system. Though costs remain high relative to other renewable technologies, these design implementations can reduce the levelized cost of electricity by over 40% compared to designs currently proposed in the literature.

9. Acknowledgements

The authors acknowledge the support of the King Fahd University of Petroleum and Minerals for funding the research reported in this paper through the Center for Clean Water and Clean Energy at MIT and KFUPM under project number R15-CW-11. Ronan McGovern acknowledges support from the Hugh Hampton Memorial Fellowship.

10. References

[1] D. A. Vermaas, M. Saakes, K. Nijmeijer, Doubled power density from salinity gradients at reduced intermembrane distance, Environmental Science and Technology 45 (16) (2011) 7089–7095.

[2] D. A. Vermaas, M. Saakes, K. Nijmeijer, Power generation using profiled membranes in reverse electrodialysis, Journal of Membrane Science 385 (2011) 234–242.

[3] P. Długołkecki, J. Dkabrowska, K. Nijmeijer, M. Wessling, Ion conductive spacers for increased power generation in reverse electrodialysis, Journal of Membrane Science 347 (1) (2010) 101–107.

[4] N. Y. Yip, D. A. Vermaas, K. Nijmeijer, M. Elimelech, Thermodynamic, energy efficiency, and power density analysis of reverse electrodialysis power generation with natural salinity gradients, Environmental Science and Technology 48 (9) (2014) 4925–4936.

[5] A. Daniilidis, D. A. Vermaas, R. Herber, K. Nijmeijer, Experimentally obtainable energy from mixing river water, seawater or brines with reverse electrodialysis, Renewable Energy 64 (2014) 123–131.

[6] D. A. Vermaas, E. Guler, M. Saakes, K. Nijmeijer, Theoretical power density from salinity gradients using reverse electrodialysis, Energy Procedia 20 (2012) 170–184.

[7] J. Veerman, M. Saakes, S. Metz, G. Harmsen, Reverse electrodialysis: A validated process model for design and optimization, Chemical Engineering Journal 166 (1) (2011) 256–268.

[8] J. W. Post, H. V. Hamelers, C. J. Buisman, Energy recovery from controlled mixing salt and fresh water with a reverse electrodialysis system, Environmental Science and Technology 42 (15) (2008) 5785–5790.

[9] D. A. Vermaas, J. Veerman, N. Y. Yip, M. Elimelech, M. Saakes, K. Nijmeijer, High efficiency in energy generation from salinity gradients with reverse electrodialysis, ACS Sustainable Chemistry & Engineering 1 (10) (2013) 1295–1302.

[10] S. Klein, F. Alvarado, Engineering equation solver, f-chart software (2014).

[11] K. Kontturi, L. Murtomäki, J. A. Manzanares, Ionic Transport Processes: in Electrochemistry and Membrane Science: in Electrochemistry and Membrane Science, Oxford University Press, 2008.

[12] R. K. McGovern, S. M. Zubair, J. H. Lienhard V, The cost effectiveness of electrodialysis for diverse salinity applications, Desalination 348 (2014) 57–65.

[13] O. Kuroda, S. Takahashi, M. Nomura, Characteristics of flow and mass transfer rate in an electrodialyzer compartment including spacer, Desalination 46 (1) (1983) 225–232.

[14] J. Chambers, J. M. Stokes, R. Stokes, Conductances of concentrated aqueous sodium and potassium chloride solutions at 25, The Journal of Physical Chemistry 60 (7) (1956) 985–986.
[15] M. Fidaleo, M. Moresi, Optimal strategy to model the electrodialytic recovery of a strong electrolyte, Journal of Membrane Science 260 (1) (2005) 90–111.
[16] R. R. A. Robinson, R. R. H. Stokes, Electrolyte solutions, Courier Dover Publications, 2002.
[17] J. Post, C. Goeting, J. Valk, S. Goinga, J. Veerman, H. Hamelers, P. Hack, Towards implementation of reverse electrodialysis for power generation from salinity gradients, Desalination and Water Treatment 16 (1-3) (2010) 182–193.
[18] R. K. McGovern, A. M. Weiner, L. Sun, C. G. Chambers, S. M. Zubair, J. H. Lienhard V, On the cost of electrodialysis for the desalination of high salinity feeds, Applied Energy 136 (2014) 649–661.
[19] E. P. Agency, Technology and cost document for the final ground water rule, http://www.epa.gov/ (October 2006).
[20] R. K. McGovern, S. M. Zubair, et al., The benefits of hybridising electrodialysis with reverse osmosis, Journal of Membrane Science 469 (2014) 326–335.
[21] E. T. Sajtar, D. M. Bagley, Electrodialysis reversal: Process and cost approximations for treating coal-bed methane waters, Desalination and Water Treatment 2 (1-3) (2009) 284–294.
[22] A. Daniilidis, R. Herber, D. Vermaas, Upscale potential and financial feasibility of a reverse electrodialysis power plant, Applied Energy 119 (2014) 257–265.
[23] M. Turek, B. Bandura, Renewable energy by reverse electrodialysis, Desalination 205 (1) (2007) 67–74.
[24] M. Fidaleo, M. Moresi, Electrodialytic desalting of model concentrated nacl brines as such or enriched with a non-electrolyte osmotic component, Journal of Membrane Science 367 (1) (2011) 220–232.

Nomenclature

Roman Symbols

A	area, m^2
C	concentration, mol/m^3
CAF	capital ammortization factor, yrs
D	diffusivity, m^2/s
F	Faraday's constant, C/mol
g	acceleration due to gravity, m/s^2
H	head loss, m
h	channel height, m
J	molar flux, mol/m^2 s
j	current density, A/m^2
K	constant
L	membrane permeability
l	length, m
$LCOE$	levelized cost of electricity, $/kWh
M	molar mass, kg/mol
NPV	net present value, $
P	power density, W/m^2
p	pressure, Pa
R	universal gas constant, J/mol K
R	resistance, Ω
r	annuity depreciation rate
$\bar{r}$	membrane surface resistance, Ω m^2
Re	Reynolds number
S	salinity, ppm
Sc	Schmidt number
Sh	Sherwood number
T	temperature, K
t	transport number
V	feed velocity, m/s
w	stack width, m

Greek Symbols

α	membrane permeability
β	mask fraction
Δ	change
ϵ	local EMF, V
ε	spacer porosity
Γ	number of periods
κ	conductivity, S/m
Λ	molar conductivity, S m^2/mol
μ	chemical potential, J/mol
ρ	density, kg/m^3
ϕ	voltage, V
π	osmotic pressure, bar
Θ	dimensionless stack resistance

Subscripts

AEM	anion exchange membrane
aq	aqueous
avg	average
c	concentrate or critical
cu	counter-ion
CEM	cation exchange membrane
CP	concentration polarization
D	density
D_h	hydraulic diameter
d	diluate
eq	equivalent
g	gross
i	inlet
L	load
m	membrane surface
mem	membrane
n	segment number
$NaCl$	salt solution
net	net
OC	open-circuit
opt	optimal
PT	pretreatment
p	pressure
s	stack
stack	stack
tot	total
w	water

Superscripts

$*$	maximizes power density

Appendix A. Validation of the gross power density model

We fit our stack model to experimental results reported in the literature. The setup employed by Vermaas et al. [1] consists of a stack of Fumatech FKS (CEM) and FAS (AEM) membranes, each 10 cm long by 10 cm wide, with 100 μm diluate and concentrate channel heights and two electrodes. The inlet feed salinities are 29,120 ppm (30 g NaCl per kg water) concentrate and 1,000 ppm (1 g NaCl per kg water) diluate.

The fitted parameters were the salt transport number t_s and the Sherwood correlation coefficient K_m (see Table E.2). The salt and water permeability L_s and L_w as well as the spacer porosity were set to conventional values for electrodialysis (see Table E.2).

In Fig. A.1, we show the ohmic surface resistance $\bar{r}_{ohm}$ validation and in Fig. A.2 we show the fit to the total equivalent stack surface resistance $\bar{r}_{eq}$. The ohmic surface resistance is the sum of the membrane surface resistances $\bar{r}_{\mathrm{AEM}}$ and $\bar{r}_{\mathrm{CEM}}$, the diluate channel surface resistance $\bar{r}_d$, and the concentrate channel surface resistance $\bar{r}_c$. The total equivalent stack surface resistance $\bar{r}_{eq}$ consists of the ohmic surface resistance $\bar{r}_{ohm}$ and losses due to concentration polarization and concentration variation along the stack:

$$\phi_{\mathrm{stack}} = \varepsilon_i^* - \bar{r}_{eq} j_{D,tot} \tag{A.1}$$

where ε_i^* is the local EMF at the inlet without including concentration polarization. The total current density is determined from load resistance matching ($R_L = \bar{r}_{eq}/wl$).

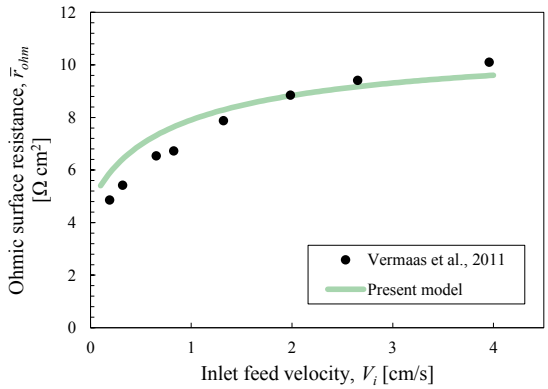

Figure A.1: Validation of the model with respect to the ohmic surface resistance $\bar{r}_{ohm}$. The root mean squared error in the fit is 0.62 Ω cm^2.

The Sherwood correlation constant, K_m, is determined by fitting an equivalent stack resistance predicted by the model to the total stack resistance reported by Vermaas et al. The currents at which the equivalent stack resistances are computed are chosen by setting the load resistances equal to the equivalent stack resistances, as in traditional load matching. The results of the fit are shown in Fig. A.2 below.

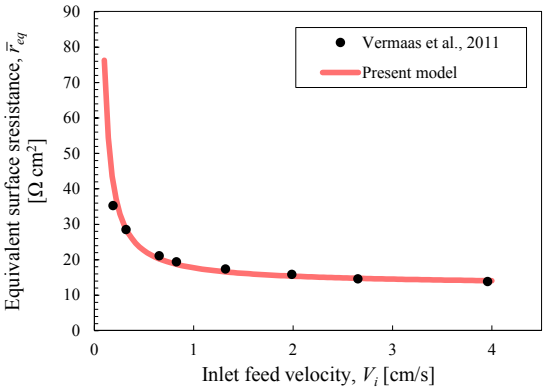

Figure A.2: Validation of the model with respect to measured equivalent stack surface resistance at various flow rates. The root mean squared error in the fit is 4.7 Ω cm^2.

The salt transport number, t_s, is then determined by fitting the gross power density predicted by the model to the gross power density reported by Vermaas et al. (see Fig. A.3 below). In our model the salt transport number captures both salt transport and current efficiency and is therefore smaller than what is reported in the literature.

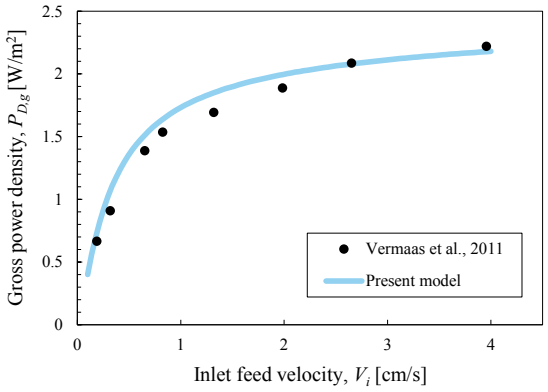

Figure A.3: Validation of the model with respect to gross power densities reported by Vermaas at various flow rates. The root mean squared error in the fit is 0.085 W/m^2.

Appendix B. Load resistance matching versus load resistance optimization

Consider the Thévenin equivalent circuit depicted in Figure B.4. The gross power density may be expressed as:

$$P_{D,g} = \left(\frac{\phi_{OC}}{R_{eq} + R_L}\right)^2 \frac{R_L}{wl} \tag{B.1}$$

where ϕ_{OC} is the open-circuit voltage (discussed further in Appendix C). When streamwise variations in

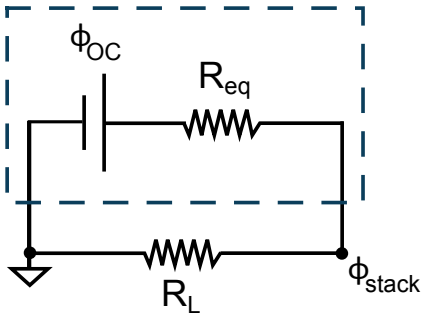

Figure B.4: The circuit shown in Fig. 4 may be reduced to a Thévenin equivalent circuit defined by the open-circuit voltage ϕ_{OC} and an equivalent stack resistance R_{eq}. The equivalent stack resistance accounts for changes in the streamwise salinity profile along the stack, see Eq. A.1.

concentration are accounted for, $R_{eq} = f(R_L)$, because changes in load resistance are coupled to changes in current and salt transport. Additionally, the open-circuit voltage is not a function of the load resistance, because the load resistance is infinite in an open circuit. Maximizing the gross power density with respect to the load resistance R_L yields the following expression for the optimal load resistance $R_{L,opt}$:

$$R_{L,opt} = \frac{R_{eq}}{2\frac{\partial R_{eq}}{\partial R_L} + 1} \tag{B.2}$$

The sign of $\partial R_{eq}/\partial R_L$ is always positive, because as the load resistance increases, the total current density decreases, reducing migrative ion transport to the diluate channel, reducing the average diluate conductivity. According to Eq. 7, this increases the diluate channel resistance, the dominant resistance in the equivalent stack resistance R_{eq}. Because $\partial R_{eq}/\partial R_L$ is always positive, the optimal load resistance is always smaller than the equivalent stack resistance.

Appendix C. Open-circuit voltage in an RED stack

The open-circuit voltage ϕ_{OC} in an RED stack with a single electrode is given by setting the load resistance equal to infinity in Eq. 8 (or equivalently, setting the total current density in the circuit $j_{D,\text{tot}}$ to zero):

$$\phi_{OC} = \frac{\sum \frac{\varepsilon_n}{\bar{r}_{tot,n}} A_n}{\sum \frac{1}{\bar{r}_{tot,n}} A_n} \tag{C.1}$$

Despite the absence of a *total* current density $j_{D,\text{tot}}$ (the sum of all local current densities through the stack), there is still a positive total salt flux into the diluate channel across the entire length of the stack (see the solid lines in Figs. C.5 and C.6). The salt flux arises for two reasons. First, regardless of the presence of local current densities, some salt diffuses into the diluate channel due to membrane imperfections (diffusive flux represented by the dotted lines in Figs. C.5 and C.6). Because there is no power extracted from or delivered to the system, the salinity profiles in both the high velocity and low velocity cases are nearly the same. Consequently, the diffusive fluxes are similar.

The flux due to migration arises from local current densities along the stack. Positive current densities form in the front half of the stack and are canceled by negative current densities in the back half. This results in positive local migration in the front half and negative local migration in the back half of the stack (see the dashed lines in Figs. C.5 and C.6).

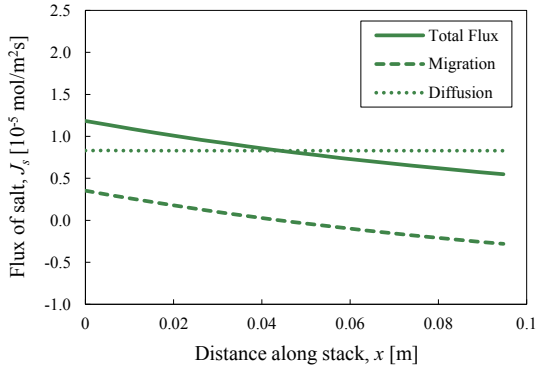

Figure C.5: Total salt flux in the low velocity (0.25 cm/s) open-circuit case, divided into a migrative flux and a diffusive flux

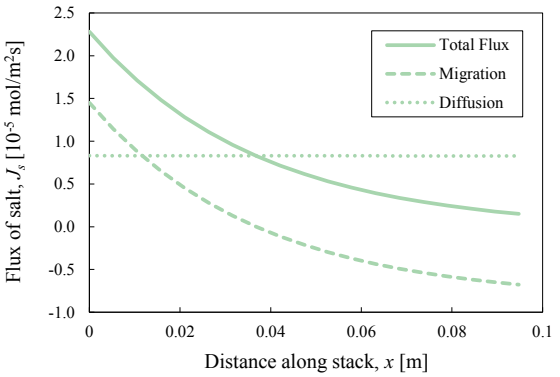

Figure C.6: Total salt flux in the high velocity (1.25 cm/s) open-circuit case, divided into a migrative flux and a diffusive flux

The reason for the rapid rise in open-circuit voltage at low velocities [2] is the rapid increase in local EMFs ε_n at higher velocities. With similar average total salt fluxes in the low and high velocity cases, there is less total salt transferred in the high velocity case, resulting in larger salinity gradients along the length and greater local EMFs. The open-circuit voltage plateaus as the total salt transferred becomes effectively zero, approaching the zero-dimensional stack.

Appendix D. Validation of the stack pumping power model

We model the pressure drop across the stack Δp as a laminar flow between two infinite plates, with a modifying constant K_p that accounts for the additional head loss caused by the spacers:

$$\Delta p = \frac{K_p \mu l V_i}{h_d^2} \tag{D.1}$$

The constant K_p was determined by fitting the model to experimental results reported by Vermaas et al. [1], see Fig. D.7 below. Multiplying by the flow rate and dividing by the active membrane area yields the stack pumping power density $P_{D,s}$ (Eq. 13).

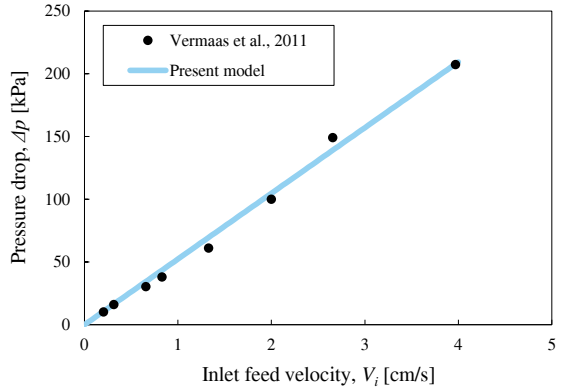

Figure D.7: The model for the pressure drop across an RED stack with 100 μm channel heights is fit to experimental results reported by Vermaas et al. [1]. A constant K_p of 293 fits the data to within a maximum error of 14%.

Appendix E. Summary of the input model parameters

A summary of the model parameters and properties is provided in Table E.2 below.

Table E.2: Membrane, solution, channel and flow, as well as costing parameters and properties used in the analysis

Symbol	Value	Ref.
Membrane/Spacer Parameters		
$C_{d,i}$	1,000 ppm	-
$C_{c,i}$	35,000 ppm	-
ϵ	0.8	[6]
Γ	20 yrs	[17]
H^a	3.66 m	[17]
t_s	0.71	Appendix A
t_w	10	[24]
L_s	1.4×10^{-8} m/s	[24]
L_w	1.4×10^{-5} mol/bar-m^2-s	[24]
$\bar{r}_{\mathrm{AEM}}$	1 Ω-cm^2	[6]
$\bar{r}_{\mathrm{CEM}}$	1 Ω-cm^2	[6]
r	6%	[17]
Solution Properties		
D_{NaCl}	1.61×10^{-9} m^2/s	[16]
μ	8.94×10^{-4} kg-m/s	[10]
Channel/Flow Parameters		
w	10 cm	[1]
h_c , h_d	100 μm	[1]
K_m	0.1	Appendix A
K_p	293	Appendix D
T	298 K	-
Cost Parameters		
K_{mem}	750 \$/m^2	[20, 21]
K_{PT}	20 \$/(m^3/day)	[17, 19]

[a] Represents the average of the measured head losses by Post et al. [17] in the summer, winter, and spring